Photon Pathlength Distributions from O_2 A-Band Absorption

Lee Harrison & Qilong Min
Atmospheric Sciences Research Center
State University of New York, Albany
100 Fuller Road, Albany, NY 12205
lee@asrc.albany.edu, min@asrc.albany.edu

Problem and Method

The issue of retrieving atmospheric photon-pathlength information from detailed spectroscopy of the O_2 band near 760 nm has been extensively studied, but to date has yielded few applications beyond the remote sensing of the surface atmospheric pressure through clear skies. Most proposed applications to the study of clouds have been for remote sensing with downward looking instruments from above. O'Brien and Mitchell (1992) describe the problem in detail and discuss previous efforts[1], with the particular view of using this passive spectroscopic method to determine cloud-top heights from satellite measurements. For their application the problem is hard due to the high accuracy required (to make the method competitive with CO_2 slicing or laser range-finding), and the fact that the pathlength distribution within the cloud represents an unwanted interference.

In this note we describe efforts that are similar in spirit to those of O'Brien and Mitchell, but for the purpose of studying the potential utility of *ground-based* spectroscopy to yield information about photon-pathlength distributions in cloudy atmospheres that would improve our understanding of absorption due to other atmospheric trace gases (e.g. H_2O) within the clouds, where the direct forward calculation depends too sensitively on geometric information about the cloud structure, that in general cannot be practically observed. For most real atmospheric cases (particularly those involving layered and otherwise inhomgeneous cloud structures) the completeness and accuracy of our radiative models cannot be tested, because too much freedom about the assumed geometry remains.

In the solar-shortwave optical domain (where the atmosphere is not at local equilibrium with the radiation) radiative transport where scattering can be neglected (such as the computation of the direct beam contribution to the normal surface irradiance) can be calculated easily from the Bougier-Beer law. In equation 1 the Bougier-Beer law is shown to the left, with I(¬) being the irradiance at a wavelength ¬, I_0(¬) the extraterrestrial irradiance, ç(¬) the product of cross-section times absorber density, and l being the appropriate atmospheric pathlength. However once scattering must be considered the problem becomes more complex; in general the distribution of pathlengths (to a particular receptor) is not known a priori. However, if we do know the distribution of pathlengths P(l) *that would occur without the presence of the particular gaseous absorber in question*, then the Bougier-Beer law has a simple extension shown to the right[2].

$$I(\lambda) \;/\; I_0(\lambda) = e^{-\chi(\lambda)\, l} \;\rightarrow\; I(\lambda) \;/\; I_0(\lambda) = \int_0^{\infty} e^{-\chi(\lambda)\, l}\, P(l)\, dl \qquad [1]$$

Of course P(l) that is the "pathlength distribution without the gaseous absorber" may seem like an unrealizeable abstraction, and further in general it must be dependent on wavelength. But nonetheless the concept has practical utility; most gas absorption of interest is very sharply

---

[1] Dr. O'Brien has given us a reference list with over 200 citations, far more than are cited in their article.

[2] For simplicity of expression geometric terms describing the product of the radiance distribution and receptor response have been omitted. Note also that P(l) will typically have finite probability density for infinite pathlengths (corresponding to photons that never reach the receptor). This is more conveniently handled by a additional coefficient always less than 1).

structured with respect to wavelength, while aerosol, cloud droplet, and surface-albedo dependent absorption have weak dependence with respect to wavelength, at least when relatively narrow ranges are considered. Thus in concept if we can infer "the" pathlength distribution by solving the inverse problem of [1], then we obtain indirect information about the cloud scattering and geometry, or may be able to apply it to the calculation of absorption at "nearby" wavelength domains.

In figure 1 we show the normalized photon pathlength probability distribution function (PDF) for the surface irradiance under the particular cloud geometry shown in the internal cartoon. We computed this result with a Monte-Carlo code modified to accumulate the PDF. Van de Hulst (1980) demonstrated that the pathlength PDF of photons returning from an infinite uniform-scattering half-space is a gamma distribution. Even before this demonstration the gamma distribution was commonly used to parameterize photon pathlengths distributions. However here is a clear example of a scene that is horizontally uniform, and yet shows a distribution that does *not* look like a simple gamma distribution. An obvious difference is that while in Van de Hulst's exact problem for an infinite half-space there can be photons returning with pathlengths negligibly larger than zero; for our transmission case no photon can have a pathlength of less than one atmosphere.

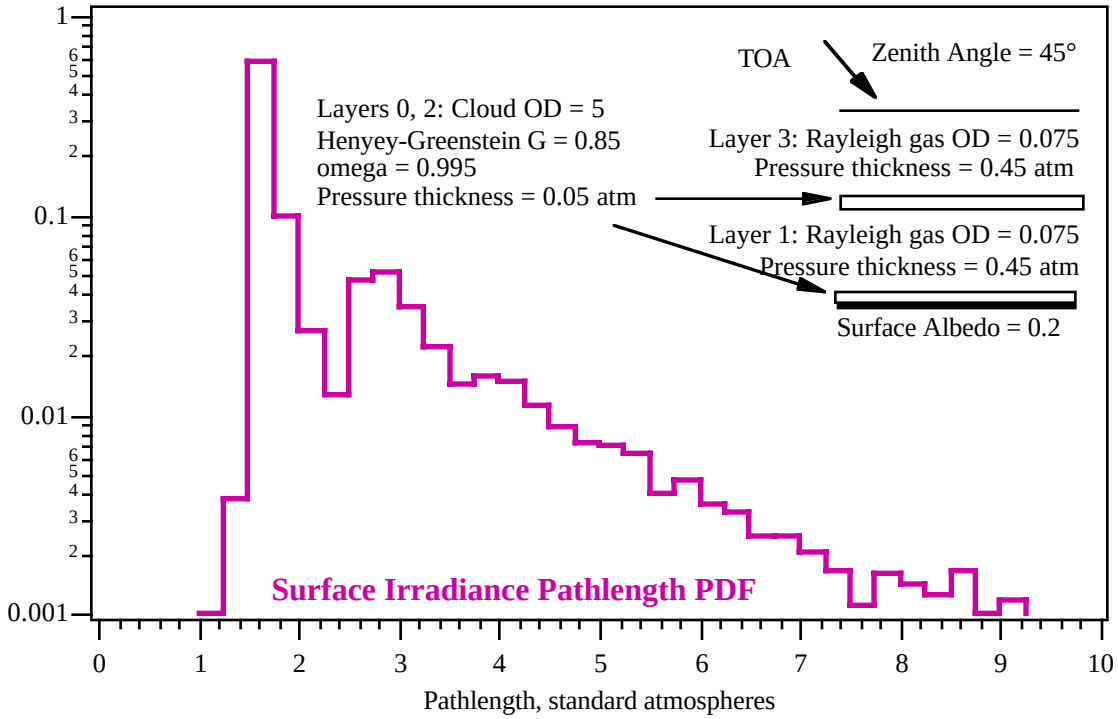

Figure 1: A photon pathlength distribution computed by a Monte-Carlo technique

Further, the distribution shown results from the sum of a series of gamma distributions, each one representing an additional round-trip between the layers 0 and 2, with increasing pathlength, broader distribution, and lesser magnitude as the order increases. Only the second is apparent; higher order ones are smeared out under the tails of the dominant shorter distributions. Much wilder PDFs are possible with cloud systems that are horizontally inhomogeneous.

So one needs to be very careful about assumptions that force reality to bend to our mathematical convenience! Nonetheless, in order to make our problem tractable in an analytic framework we followed the general method described by Bakan and Quenzel (1976), but with simple modifications appropriate for our terrestrial problem. Their method does assume that the distribution is a function including the gamma distribution, and takes advantage of the fact that an analytic Laplace transform exists therefore. Since the right equation 1 is a scaled Laplace transform

of the PDF, computation of the inverse problem is straightforward. Our immediate goal is to determine the optical performance needed to achieve useful accuracy for inverted or inferred results; for this purpose the analytic problem can provide useful tests of synthetic cases that conform to it's assumptions. The instrument performance needed to achieve reasonably accurate results for these test cases can then be considered as the minimum performance needed for an instrument of this kind.

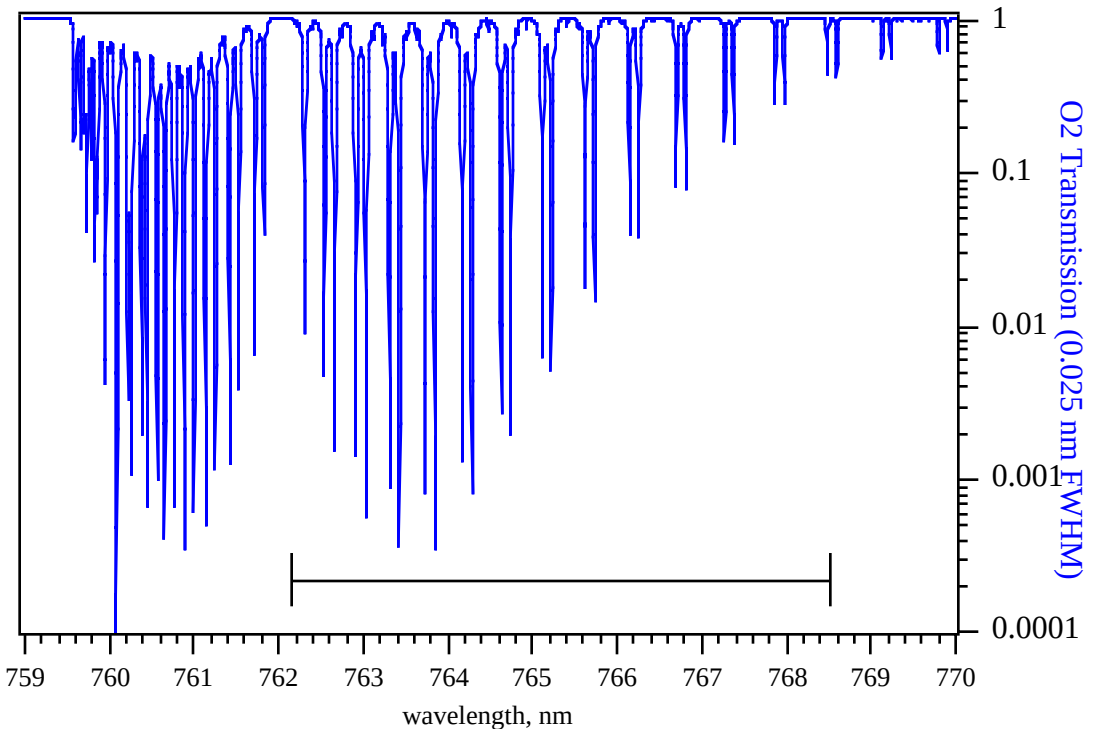

Figure 2: Transmission of one atmosphere of O_2.

Figure 2 shows the A-band of O_2, taken from HITRAN computations for the transmission through 1 standard atmosphere, and then convolved to a triangular optical slitwidth of 0.025 nm FWHM. The abscissa is shown in wavelength, and so this figure appears "reversed" for those of you accustomed to seeing these data in wavenumber; the P branch is at longer wavelengths. All our computations were done using the domain in the P branch shown by the horizontal brace; we chose this domain because the "looser" spectrum of the P branch eases instrument resolution requirements compared to the R-branch, and it represents a span in wavelength we consider practical for a dispersive instrument with a discrete-array detector.

For our computations of synthetic spectra we used line parameters from Burch and Gryvnak (1969). These data were chosen because they were easily accessible to us. They may not be so accurate as more modern data used for HITRAN or MODTRAN3, but we could not obtain either of these databases. For the purposes of the sensitivity studies shown here the accuracy of the spectroscopic data base is not critical; it need merely serve as a useful analog of the real problem.

In our atmosphere Doppler broadening is negligible compared to collisional broadening. Consequently we (and all other papers on this subject we have read) assume that line shapes are well described as Lorentzian. The behavior is shown in equation 2, and in dimensionless form with respect to $\sqrt{} / \sqrt{}_i$ in figure 3.

$$k_i = \frac{S_i}{\pi} \frac{\alpha_i}{(\upsilon - \upsilon_i)^2 + \alpha_i^2} \quad where \ \alpha_i = \alpha_i^0 \frac{p}{p^0} \left(\frac{T^0}{T}\right)^{1/2} \qquad [2]$$

Note further that when far from the line center, such that $(\upsilon - \upsilon_i) >> \alpha_i$, this function simplifies to equation 3.

$$k_i = \frac{S_i}{\pi} \frac{p}{p^0} \left(\frac{T^0}{T}\right)^{1/2} \frac{1}{(\upsilon - \upsilon_i)^2} \qquad [3]$$

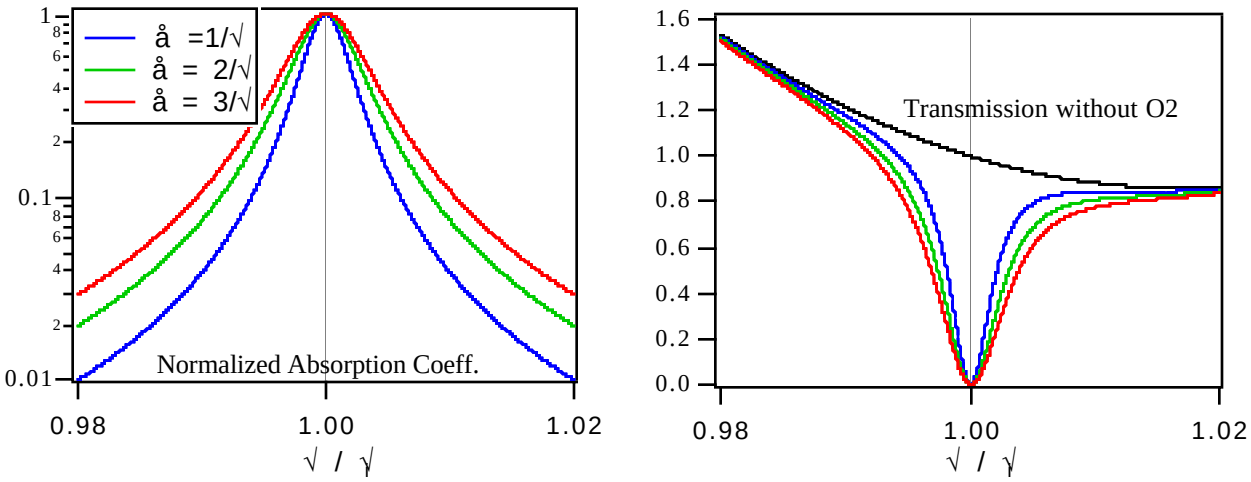

Figure 3: Lorentz profiles in absorption and transmission.

Bakan and Quenzel (1976) depend on the existence of the Laplace transform

$$\int_0^\infty x^b e^{\alpha x} e^{-kx} dx = \frac{\Gamma(b+1)}{(k-\alpha)^{b+1}}$$

for our efforts we must modify this to allow a path distribution with zero probability for lengths shorter than the atmospheric depth. To do so we simply introduce $x = x' - l_0$, and then the result is a consequence of the general shift operator for the Laplace transform

$$\int_0^\infty (x' - l_0)^b e^{\alpha(x' - l_0)} e^{-kx'} dx' = \frac{\Gamma(b+1)}{(k-\alpha)^{b+1}} e^{-kl_0} \qquad [4]$$

While in these expressions the choice of symbols is arbitrary, k will be given the meaning of k in equation 3. α, b, and l_0 are arbitrary coefficients that select a particular distribution. With these results in hand we have the recipe for all calculations shown below: an arbitrary pathlength distribution described by α, b, and l_0 (or a linear combination of more than one) is assumed. Using the line parameters from Burch and Gryvnak (1969), and equations 1 and 2, a "forward" calculation of the predicted spectrum is made to arbitrary spectral resolution. This spectrum can then be convolved with any proposed instrument slit-function, and instrument noise or other errors (such as wavelength mis-registration) can be applied. Hereafter we will call this the "pseudo-observation."

Simultaneously, from equation 2 and the line-parameter database, a value of k can be computed for every wavelength $\Re$, as the sum of the k_i. Note that any particular value of k may come from many differing points within the observed spectral domain. From equation 4, and identically analogous to Bakan and Quenzel, we then simply find the best fit of our pseudo-observation transmissions vs. k, to the algebraic form (or sum of multiple occurrences)

$$T(k) = \frac{A}{(Bk + 1)^C} e^{-k l_0} \qquad [5]$$

where A, B, C are free parameters, and l_0 may either be treated as a free parameter, or set to one atmosphere. In our case we find these parameters by non-linear least-squares regression. With these the inverse estimate of the original pathlength distribution can be reconstructed from the pseudo-observations trivially as (again, there may be linear combinations):

$$P(x) = \frac{A}{B^C \Gamma(C)} (x - l_0)^{C-1} e^{(x - l_0)/B} \qquad [6]$$

where P(x) is the differential probability of the path length x, and all other terms are as above.

Results

Figures 4 and 5 show the results of varying slit-function widths on the retrieval of plausible single-mode and double-mode distributions. The latter is a linear combination of two distributions. In both cases first calculations were done using only the data in the spectrum where $10^{-3} \le k \le 10$ and then repeated with $10^{-2} \le k \le 6$ (no significant differences are observed); 1% of-signal uniform-random deviates in transmission were superimposed on the synthetic spectrum.

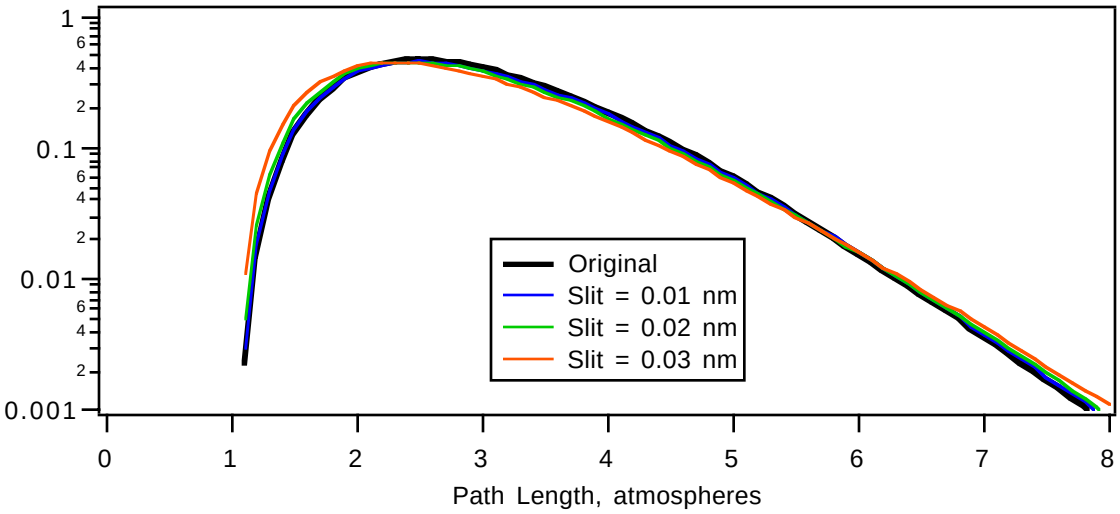

Figure 4: A single-mode PDF distribution, and retrieval thereof from the pseudo-observations with varying slit-function widths.

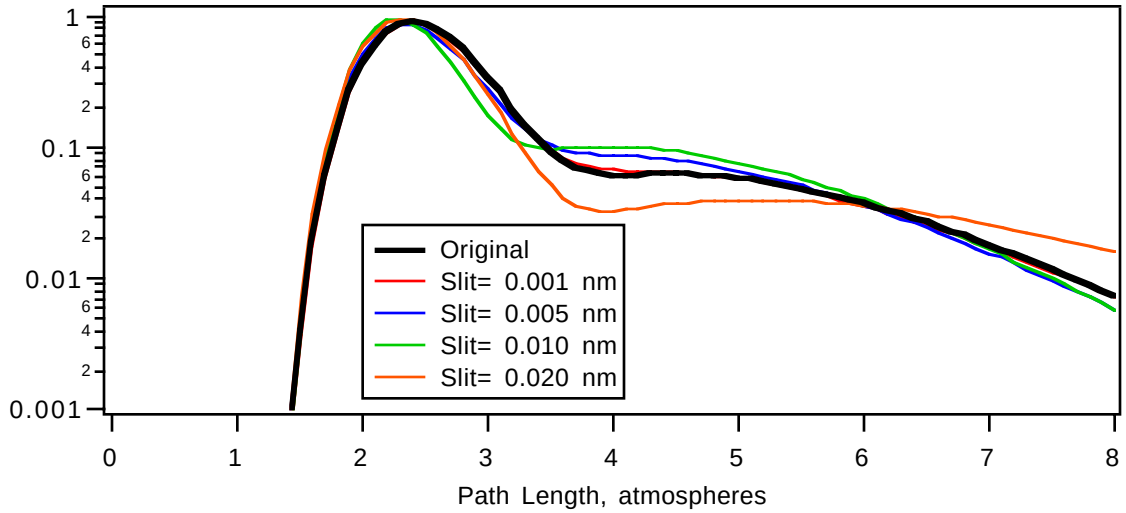

Figure 5: A double-mode PDF distribution, and retrieval thereof from the pseudo-observations with varying slit-function widths.

We can now determine the sensitivity of the retrieved pathlength distributions to various classes of potential instrument errors. We have done more than can be shown here, and have further work to do before we will be ready to consider instrument design tradeoffs. However the following figures, all showing errors that accrue to the distribution shown in figure 4 as a result of potential instrument errors, are instructive. The distribution shown in figure 4 has a mean pathlength of 3 atmospheres, and a standard deviation of 1.6.

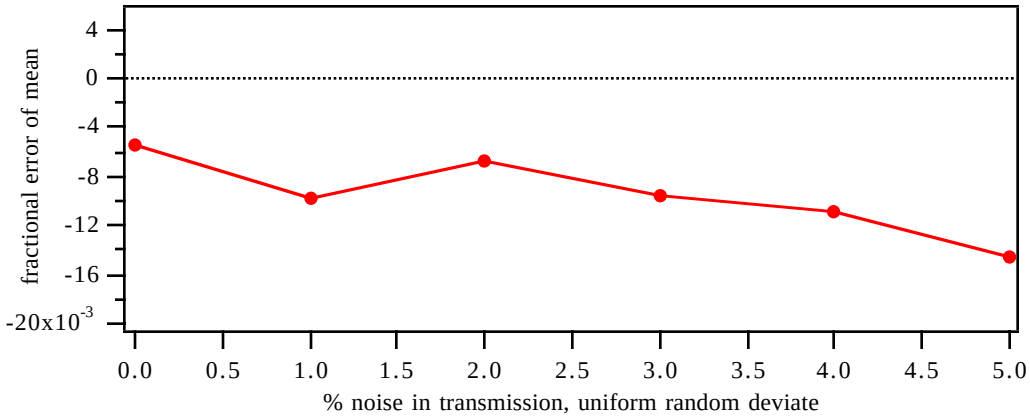

Figure 6: Fractional error of mean pathlength as a function of noise in the transmission measurement

In figure 6 we see that this retrieval always slightly underestimates the mean, but that this error is not very sensitive to *random* errors in transmission, for errors that we think plausible. The results are never worse than approximately 1.5%. Although they are not shown here, a *bias* error in the transmission can have a much more serious effect on the retrieval, and will be a major factor in instrument design. Bias in the estimate of the transmission will largely arise as a result of the necessity of interpolating the "zero O_2 absorption" signal across the A-band (see the right-side panel of figure 3), from measurements of transmission to either side. This in turn will depend on the accuracy and stability of the individual-pixel responsivities, that we cannot address at this time. However the effect of signal bias

becomes more pronounced as k becomes smaller, and thus may impose a lower bound on the values of k that can be used for the retrieval.

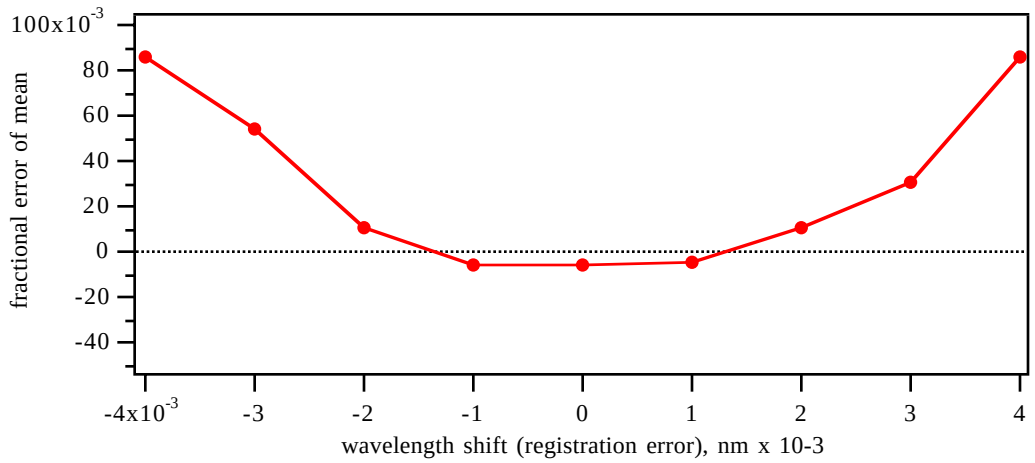

Figure 7: Fractional error of mean pathlength as a function of wavelength mis-registration

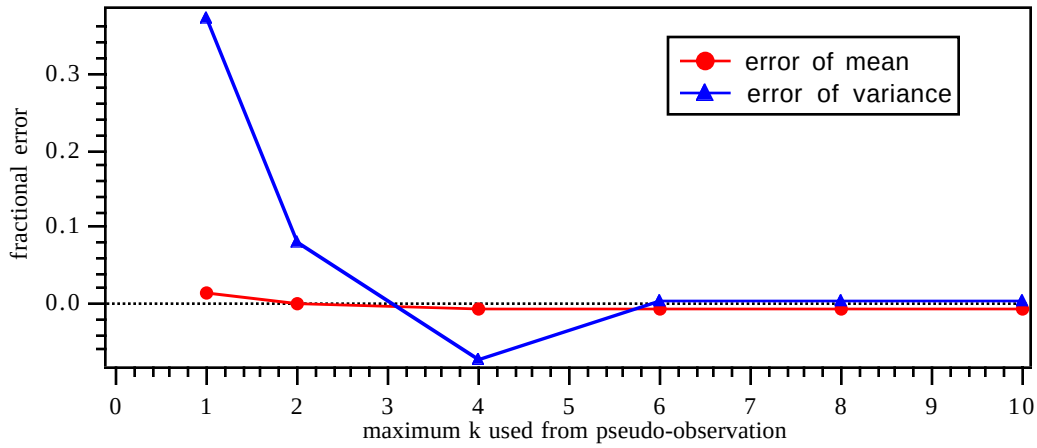

Figure 8: Fractional error of mean pathlength and variance as a function of the maximum k that can be observed

Figure 7 shows that wavelength registration accuracies of approximately 0.002 nm are needed for wavelength error to make a negligible contribution to errors in the inferred mean pathlength. Errors in the inferred pathlength grow rapidly for wavelength mis-registrations significantly larger than this. Note that it may be possible to adjust the wavelength scale of an observed spectrum by peak-fitting to ease what otherwise is a stringent instrument design constraint, but we do not consider this issue further here.

Figure 8 shows that retrieving the variance of the distribution depends to a much greater degree on being able to use higher values of k than does the retrieval of the mean. This sets a instrument specification for out-of-band rejection. From the graphs we see that we need $k \geq 5$ to obtain an accurate estimate of the pathlength variance; if out-of-band light were not to contribute more than 1% of stray light to a measurement at k = 6 then the out-of-band rejection ratio would need to be 6×10^{-5}.

This goal is beyond the state of the art for single Fabry-Perot interferometers, but can be done at these wavelengths by carefully engineered grating spectrometers.

Conclusions

For the purposes of testing radiative transfer models for cloudy sky conditions against observations information about the photon pathlength distribution would be useful to set constaints on the cloud geometries being considered. Such data can in principle be acquired by ground-based spectroscopy of the O2 A-band absorption. This goal is more tractable from an instrument and inversion point of view than is the problem of accurate cloud-top height retrieval from downward-looking spectroscopy, primarily because a lower accuracy of inference remains scientifically useful.

The methods shown here allow the rapid assessment of realistic error budgets for potential instruments intended to retrieve pathlength distribution information from A-band spectroscopy. These methods may also prove useful as actual inversion methods if only limited parametric information about the distribution (e.g. first two moments) are to be retrieved.

The mean pathlength can be retrieved from low-resolution data, and is relatively insensitive to many other errors. Higher order moments, or equivalently the detection of pathlength distributions that have multiple modes, require much better instrument performance. Efforts to retrieve more than a few moments of the pathlength distribution appear to be beyond what can be supported by practical instruments. Similar conclusions are likely to be true (but have not been proved) with respect to efforts to obtain pathlength profiles, or other data requiring the retrieval of many free parameters.

References

Bakan, S. and H. Quenzel (1976) "Pathlength Distribution of Photons Scattered in Turbid Atmospheres," Bei. Phys. Atmos. 49: pp 272-284

Burch, D.E. and D.A. Gryvnak (1969) "Strengths, Widths, and Shapes of the Oxygen Lines near 13,100 cm^{-1} (7620 nm)" Appl. Opt. 8, 1493-1499

O'Brian, D.M., and R.M. Mitchell (1992), "Error Estimates for Retrieval of Cloud Top Pressure Using Absorption in the A Band of Oxygen" J. Appl. Met. 31, pp 1179- 1192

Van de Hulst, H.C. (1980) Multiple Light Scattering. Tables, Formulas, and Applications: Volume 1, Academic Press